This is a repository copy of *Effect on the spectral purity of photon-pairs due to on-chip temporal manipulation of the pump*.

White Rose Research Online URL for this paper:
https://eprints.whiterose.ac.uk/221511/

Version: Published Version

Effect on the spectral purity of photon-pairs due to on-chip temporal manipulation of the pump

Lukas Rodda ⓘ ; Ben M. Burridge ⓘ ; Jorge Barreto ⓘ ; Imad I. Faruque ✉ ⓘ

Check for updates

View Online

Export Citation

Articles You May Be Interested In

Quantum states generation and manipulation in a programmable silicon-photonic four-qubit system with high-fidelity and purity

APL Photonics (July 2024)

Backscattering in nonlinear microring resonators via a Gaussian treatment of coupled cavity modes

APL Photonics (June 2021)

On-chip heralded single photon sources

AVS Quantum Sci. (October 2020)

Effect on the spectral purity of photon-pairs due to on-chip temporal manipulation of the pump

View Online   Export Citation   CrossMark

Lukas Rodda,[1]   (ID)   Ben M. Burridge,[1,2]   (ID)   Jorge Barreto,[1]   (ID)   and Imad I. Faruque[1,a]   (ID)

AFFILIATIONS

[1] Quantum Engineering Technology Labs, University of Bristol, Nanoscience and Quantum Information Building, Tyndall Avenue, Bristol BS8 1FD, United Kingdom

[2] Quantum Engineering Centre for Doctoral Training, Centre for Nanoscience and Quantum Information, University of Bristol, Bristol, United Kingdom

[a] Author to whom correspondence should be addressed: imad.faruque@bristol.ac.uk

ABSTRACT

Photonic Integrated Circuits (PICs) are a promising contender for quantum information technologies. The spectral purity of photons is one of the key attributes of photon-pair sources based on nonlinear optics. We can obtain >99% purity in PIC ring-resonator photon-pair sources by manipulating the pump pulse in the time domain. Here, we have developed a PIC to shape a pulse into dual, triple, and quadruple pulses and investigated the effect of these pump pulse configurations on the purity. Our results show that more complex configurations, compared to a two-pulse configuration, do not result in comparatively higher purity but allow more accurate control over choosing arbitrary values of the purity.

I. INTRODUCTION

Quantum information is the foundation for many strategic technologies, such as quantum computing and communication.[1–4] Integrated photonics has shown to be a promising platform to scale-up and stabilize quantum experiments while benefiting from well-developed fabrication techniques.[5] Using photons as quantum bits (qubits) requires a source of single photons, such as a heralded single-photon source. Recently published results have presented various methods to improve the spectral purity of photon sources, which is crucial for high-fidelity gate operation.[6] For example, complex resonator designs[7] and temporal manipulations of the pulsed pumps[8,9] are two of the ways to achieve near unity purity, an essential characteristic of photon pair sources for heralding.

Nonlinear light–matter interaction mechanisms such as spontaneous four-wave mixing (SFWM) are often used in photonic devices in integrated photonics platforms (e.g., a silicon-on-insulator platform) to generate photon-pairs, where two pump photons are converted into a signal and an idler photon. A ring-resonator is one such structure that enhances the production of photon-pairs with high brightness and high purity.[6] The spectral purity of this source is often quantified using the joint spectral amplitude (JSA) of the emitted signal and idler photons. This is given by Ref. 9, adapted to suit our use,

$$\Phi(\omega_s, \omega_i) = \int d\omega_p d\omega_{p'} \alpha(\omega_p)\alpha(\omega_{p'})\phi(\omega_p, \omega_{p'}, \omega_s, \omega_i)$$
$$\times L(\omega_p)L(\omega_{p'})L(\omega_s)L(\omega_i), \quad (1)$$

where $\alpha(\omega)$ is the pump envelope, ϕ is the phase matching term, and $L(\omega)$ is the Lorentzian field enhancement terms arising from the ring resonances, with the pump, signal, and idler frequencies: ω_p, ω_s, and ω_i. The pump is spectrally confined by the ring resonance at the pump frequencies, which causes correlations in the photon pairs. Theoretically, the purity of a photon pair state generated in a ring is limited to 0.92 for a single pulse pump.[10] However, by manipulating the phase and temporal spectrum of the pump, the effect of the resonance at the pump frequencies can be removed, leading to a separable pair state and arbitrarily high purity,[8]

$$\alpha_{target} \propto L(\omega_p)^{-1} \times \alpha_{single}. \quad (2)$$

This ideal target pump can be approximated using a dual pulse [Fig. 1(a)] of two π phase-shifted pulses, which has been theoretically
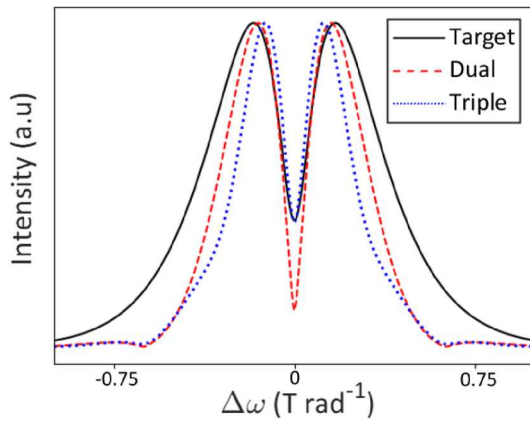
FIG. 1. Target pulse for completely pure JSA, compared to dual and triple pulse pumps. The dual pulse shown has a splitting ratio of 0.55 and a delay of 10 ps, the best performing case. The triple pulse has splitting ratios of 0.8 and 0.8 and a 10 ps delay between each pulse.

shown to improve purity past 0.99[8] and was demonstrated experimentally using fiber optics.[9] However, the pump configurations were only stable for a relatively short period of time, and the tuning ranges of the parameters were limited—only a π phase difference can be chosen, and setting the amplitudes was cumbersome.

Here, we present the simulated and experimental results, which explore alternate pump profiles, such as a pump containing three pulses to, therefore, match, improve, or provide more control over the purity of a dual pulse pump. We designed and used a PIC, which allows multiple pump pulse configurations compared to the literature[9,1] and granular control over parameters while guaranteeing the phase stability of the composite pump pulse. The pump can then be used with any conventional resonator source, allowing easy integration into new or existing photonic experiments. Our theoretical results are all numerically calculated over a large number of parameter spaces of our experiment.

II. METHODS

The setup shown in Fig. 2(a) was used to create various pulse pump configurations and record the spectral purity of our photon pair source. Our experiment uses two 220 nm thickness silicon-on-insulator chips with a waveguide cross-section of 500×220 nm^2, the first: the pulse shaping chip, fabricated by CORNERSTONE, and the second: the resonator source chip, reported in Ref. 11, which is fabricated by AMF, Singapore. We used a pulsed laser (PriTEL FFL) that produces *sech* shaped single pulses at a 1546.12 nm wavelength with a 41 GHz Full-Width at Half Maximum (FWHM) and a 50 MHz repetition rate. Such a pulse pump α_{single} is described using the following equation:

$$\alpha_{single} = sech((\omega - \omega_0)/\sigma), \quad (3)$$

where ω denotes the angular frequency, ω_0 denotes the central frequency, and σ denotes the FWHM of the pulse. These pulses were coupled to the first chip, denoted as the pulse shaping chip in the figure, using a polarization controller to optimize the coupling into

the chip using a vertical grating coupler and a beam splitter as a 10% tap to monitor the input power in the chip.

Each single pulse is split into two using a Mach–Zehnder interferometer (MZI). The MZI is controlled using a thermo-optic phase shifter to obtain the desired splitting ratio η_1. The two pulses are then temporally separated using a fixed delay ($\Delta\tau_1$) line of 20 ps ($\Delta\tau_1$ = 20 ps) and then recombined using another MZI. The relative phase difference (ϕ_1) between the two pulses can also be set using another thermo-optic phase shifter. At this point in the circuit, the resulting pulse configuration can be expressed by the following equation, which can be denoted as a dual pulse:

$$\alpha_{dual} = \left[\sqrt{\eta_1} + \sqrt{1 - \eta_1} \exp\left(-i\Delta\tau_1(\omega - \omega_0) + i\phi_1\right) \right] \times \alpha_{single}. \quad (4)$$

The same process continues in series twice more before the resulting pulse is output from the chip, allowing a pulse configuration of up to four pulses to be created with arbitrary splitting ratios and phases and with fixed 20 ps time delays between them. Therefore, a triple pulse with another splitting ratio (η_2), time delay ($\Delta\tau_2$), and phase (ϕ_2) can be expressed as

$$\alpha_{triple} = \left[\sqrt{\eta_1} + \sqrt{(1 - \eta_1)\eta_2} \exp\left((-i\Delta\tau_1(\omega - \omega_0) + i\phi_1\right) \right.$$
$$\left. + \sqrt{(1 - \eta_1)(1 - \eta_2)} \exp\left(-i\Delta\tau_2(\omega - \omega_0) + i\phi_2\right) \right] \times \alpha_{single}, \quad (5)$$

where all delays and phases are relative to the first pulse maximum.

A few configurations are plotted in Fig. 2(b), where the single pulse, Eq. (3), was numerically fit to the corresponding output of the chip, and the dual and triple pulses, Eqs. (4) and (5), were fit using the same values for η, $\Delta\tau$, and ϕ as those set on the chip. The coupling loss from the chip to the fiber using a grating coupler is 10 dB. Once the desired pulse configuration was acquired, it was amplified using an erbium-doped fiber amplifier (EDFA) to be used as a strong laser pump for stimulated emission tomography (SET) in the second chip.[12] A VOA was used to bring the power to an arbitrary level, and an extra dense-wavelength division multiplexer (DWDM) was used to filter the noise after the EDFA. This was then coupled into the second chip, with a 1% tap to monitor the combined power and two PCs to optimize the coupling.

The second chip contains a racetrack resonator source with a Q-factor of 26 000, which can produce photon-pairs through a nonlinear light–matter interaction through SFWM. To perform SET, we have combined our pump laser (1546.12 nm) with a continuous wave (CW) laser (Yenista TUNICS) as a seed field (1543 nm) using a DWDM [Fig. 2(a)].

The racetrack resonator is followed by an asymmetric-MZI that removes the pump field from the signals. The pump and the stimulated idler fields were combined with a final DWDM, which filtered out the seed field. The intensity of the generated idler photons was measured using a (Finisar WaveAnalyser) optical spectrum analyzer (OSA). Here, the input powers for the pulsed pump and the CW signal field are 6 mW and 5–15 mW, respectively, and the idler field output was recorded between 3 and 10 mW, depending on the pump configuration. As our outcoupling loss was 8 dB per signal/idler channel, the raw heralding efficiency for a single pulse is estimated as −19 dB (1.3%) at the detectors.

A single pulse Joint Spectral Intensity (JSI) was collected using SET first by configuring the pulse shaper circuit so that the original
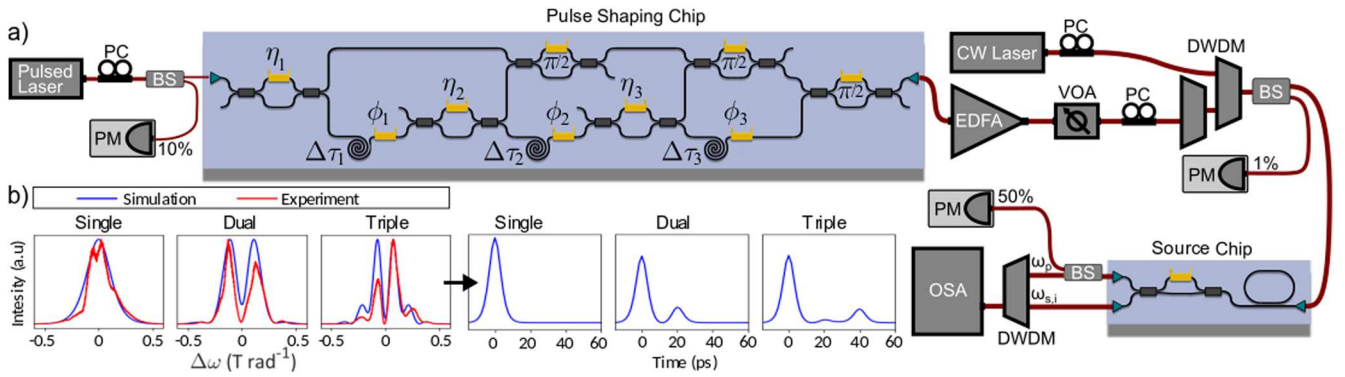
FIG. 2. (a) Experimental setup. Pulses from a laser enter the first chip, which generates pump profiles. These are combined with a stimulating signal field from a continuous wave (CW) laser to generate a stimulated idler field in a ring resonator source on the second chip. An optical spectrum analyzer (OSA) then measures the idler field. PC: polarization controllers, BS: beam splitters, PM: power meters, EDFA: erbium-doped fiber amplifier, VOA: variable optical attenuator, and DWDM: dense-wavelength division multiplexer. (b) Single, dual, and triple pulses from experimental and simulated data, where the experimental data were collected using the OSA after setting the parameters on-chip, and the simulated data were obtained from models using the same parameters. For the dual pulse, $\eta = 0.8$ and $\Delta\tau = 20$ ps [modeled with Eq. (4)]. For the triple pulse, $\eta_1, \eta_2 = 0.8, 0.2$ and $\Delta\tau_1 = 20$ ps, $\Delta\tau_2 = 40$ ps [modeled with Eq. (5)]. An inverse Fourier transform was used to plot the simulated pulses in the time domain. The slight mismatch between the measured and simulated pulses was due to the broad linewidth of the pulsed (>500 pm) laser drifting from the central frequency; however, the spectral region of the resonances (60 pm) is small and, therefore, this slight mismatch does not make a significant difference in the purity of the resonator.

pulse was not split. Then, a triple pulse was created by splitting a single pulse twice with a ratio of $\eta_1 = \eta_2 = 0.8$, and the JSI was collected.

The JSA is approximated using experimentally measured $\sqrt{JSI}$. Alternatively, we simulate the JSA numerically in MATLAB with Eq. (1) and the corresponding pulse shape (α). We then calculate the purity for each pulse pump configuration through a Schmidt decomposition of the JSA.[10] We have also simulated the in-resonator field spectral distribution given by $A_p(\omega) = L(\omega - \omega_p) \times \alpha_{pump}[(\omega - \omega_p)]$ and the corresponding temporal distribution using Fourier transformations.

III. RESULTS

The pulse shaper circuit was characterized by creating single, dual, and triple pulse pumps with varying splitting ratios, phases, and delays. These matched up well with our model [Fig. 2(b)], showing the chip is capable of a fine level of control. The single, dual, and triple pulse pumps were modeled with Eqs. (3)–(5).

An n pulse pump was modeled to investigate the purity of a pump with an arbitrary number of pulses. A train of pulses was constructed by adding n single pulses together with a constant time delay between them, all π out of phase with respect to the first pulse. Then, two different configurations, in terms of the pulse amplitudes, were used. First, the pulse train was set so that after an initial pulse, each next pulse had a constant, lower amplitude, as shown in Fig. 3(a). Then, a pulse train was set, where the amplitude of each subsequent n pulse was reduced using a splitting ratio of $\eta/2^n$, as shown in Fig. 3(c), similar to how the pulse shaper circuit operates. The JSA of a resonator source was simulated numerically with Eq. (1), allowing the purity to be calculated for each pulse pump configuration.

Both configurations showed similar results [Figs. 3(b) and 3(d)]. No improvement in purity over the dual pulse case was seen
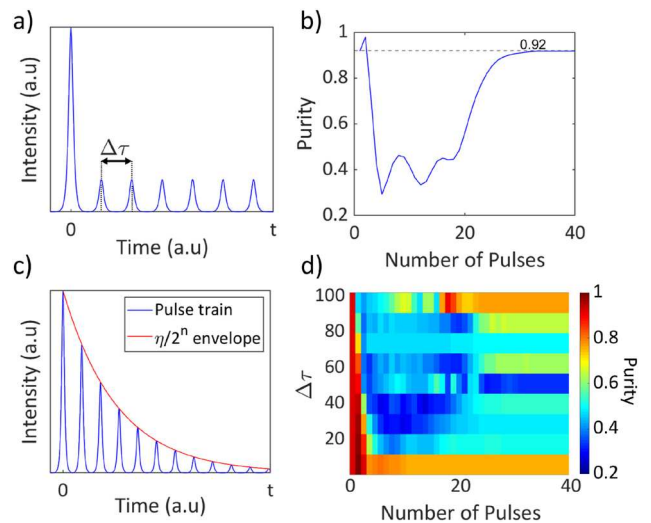

FIG. 3. (a) An example of a pulse train used in the n pulse pump simulations. Here, the amplitude is constant after an initial stronger pulse, with a time delay $\Delta\tau$ between each pulse. (b) Purity from simulated JSAs as the number of pulses increases for the constant pulse train. (c) Pulse train where amplitude decreases according to a splitting ratio η for each pulse n, as shown by the envelope. (d) Purity as the number of pulses increases, with different delays ($\Delta\tau$) between them. Here, the pulse train amplitudes decreased according to a splitting ratio $\eta = 0.55$, as shown in (c).

as the number of pulses increased. Furthermore, only a few cases exceed the 0.92 purity limit, with the first configuration only plateauing at the limit as the pulse train approximated a single pulse. Since these configurations have fixed time delays and phases, to find higher purity solutions, we focus on the triple pulse configuration [Eq. (5)], where the splitting ratios and phases can be varied arbitrarily to

10 January 2025 11:57:34

explore a larger parameter space to illustrate any benefits over the dual pulse case.

First, the two splitting ratios $(\eta_{1,2})$ were varied while keeping the delays $(\Delta\tau_{1,2})$ and phases $(\phi_{1,2})$ constant at 20 ps and π, respectively. Then, η_1 and η_2 were both fixed to 0.8, and the phases were varied, keeping the delays the same. The parameters were scanned, simulating the JSA for each configuration, creating two heatmaps, as shown in Fig. 4.

The results show (Fig. 3) that the purity does not reach higher than the best dual pulse case, and only a few configurations perform better than the single pulse limit. For simulations of the dual pulse [Eq. (4)], the best performing configuration reaches a purity of 0.999, with a large set of the parameter space going above 0.99.[8] On the other hand, almost all of the space for the triple pulse gives purity at or below the 0.92 limit, with only a small area in the phase simulation reaching higher than 0.95. However, this shows that a wide range of purity values can be selected simply by changing the phase and splitting ratios, with high tolerance. This is another benefit of the integrated circuit, where trivially changing the on-chip parameters allows a fine level of control over the pump profile and, therefore, the purity.

Figure 5 presents the simulated and experimental data collected for a chosen triple pulse case to show the reduction in purity when a third pulse is added. To establish a baseline with our experimental setup, we first recorded the JSI for a single pulse, as shown in Fig. 5(a), which agrees with the simulated purity [Fig. 5(c)]. As seen from the simulation, any triple pulse should show a 0.92 or lower purity when both phases are set to be π out of phase. Here, η_1 and η_2 were set to 0.8 to improve the signal-to-noise ratio of the measured JSI. The result shows an estimated purity of 0.845, which is very close to the simulated purity of 0.828, where slightly higher purity in the experimental case arises from a small but not insignificant noise floor. A higher purity (98%) JSI data was also experimentally recorded (see the supplementary material). This noise floor was around 90 dBm and was mitigated by using an average of 64 recorded datasets.

We have simulated the in-resonator field (A_p) to understand the reduction in purity when more than two pulses are used. Figure 6 depicts the spectral and temporal pump distribution inside the resonator source. The spectral distribution is given by $A_p(\omega) = L(\omega - \omega_p) \times \alpha_{pump}[(\omega - \omega_p)]$, and the temporal distribution is obtained by using Fourier transformations. This figure shows
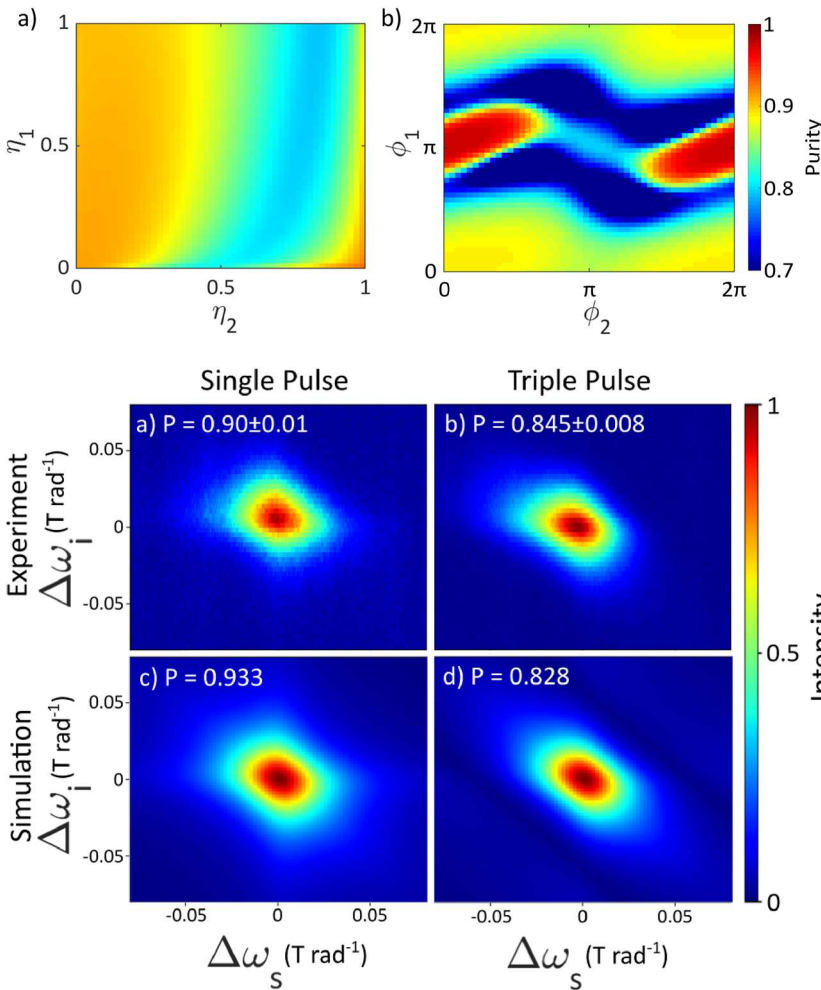

FIG. 4. (a) Purity as splitting ratios η_1 and η_2 are varied for a triple pulse with $\Delta\tau_1$ and $\Delta\tau_2$ set to 20 and 40 ps, respectively, and ϕ_1, ϕ_2 both set to π. (b) Purity as the phases of the second and third pulses are varied relative to the first pulse. Here, η_1 and η_2 are both 0.8, with the same delays as previously mentioned.

FIG. 5. Experimentally collected JSIs and the calculated purity P for a single pulse (a) and a triple pulse (b) with $\eta_1 = \eta_2 = 0.8$ and $\Delta\tau_1 = 20$ ps, $\Delta\tau_2 = 40$ ps. Panels (c) and (d) show the simulated JSIs for the same single and triple pulse configurations modeled using Eqs. (3) and (5).
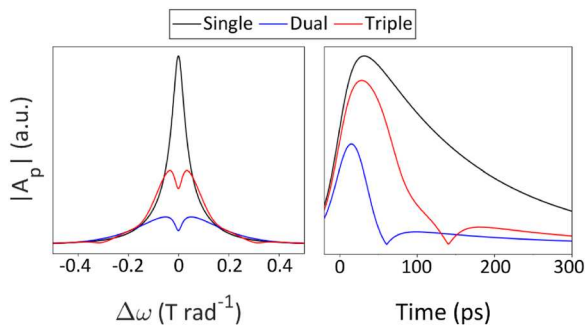
10 January 2025 11:57:34

FIG. 6. Simulated in-resonator pump fields for single, dual, and triple pulse pumps in (a) the frequency and (b) time domains, with dual pulse configurations of $\eta = 0.55$ and $\Delta\tau = 10$ ps and triple pulse configurations of $\eta_1 = \eta_2 = 0.8$ and $\Delta\tau_1 = 20$ ps, $\Delta\tau_2 = 40$ ps.

that the right configuration of the dual pulse matches best the target spectral shape (Fig. 1), while a triple-pulse adds extra lobes. Adding the second pulse in the dual-pulse configuration significantly reduces the temporal pump energy inside the resonator, as denoted by the zero-crossing point, therefore, effectively broadening the pump resonance and improving purity. A third pulse with the same phase as the second adds significantly more energy to the residual energy from the second pulse, and hence, the effective reduction in purity. While this can be alleviated somewhat by adjusting the phases, the dual pulse still has a quicker energy reduction. The triple pulse pumps investigated can get close to the desired target pump, but the right dual pulse can fit better, as shown in Fig. 1, meaning a dual pulse results in higher purity than any of the tested triple pulses.

IV. CONCLUSION

This work investigated the temporal manipulation of a pulsed pump with more than two pulses, both through simulation and by using a photonic integrated circuit experiment, on the spectral purity of a ring resonator photon-pairs source. Our results indicate that there was no gain in purity for any pump with more than two pulses for any of the pump profiles investigated. A dual pulse pump provides the best intrinsic match for a specific target pump shape, which would result in theoretically maximum purity. An advantage found with the triple pulse is an accurate level of control: with more parameters that are easily adjustable experimentally, the purity can be selected within a large range to any desired value.

However, here the parameters investigated were chosen based on results from the existing literature.[8,9] In the future, a larger parameter space could be more rigorously explored, either corroborating these results or finding outliers with higher purity with comparatively high brightness.

SUPPLEMENTARY MATERIAL

See the supplementary material for information on the resonances and transmission spectra of the ring resonator used in this experiment.

AUTHOR DECLARATIONS

Conflict of Interest

The authors have no conflicts to disclose.

Author Contributions

Lukas Rodda: Formal analysis (equal); Investigation (lead); Methodology (lead); Software (lead); Visualization (lead); Writing – original draft (equal); Writing – review & editing (supporting). **Ben M. Burridge**: Conceptualization (equal); Methodology (equal); Software (supporting); Supervision (supporting). **Jorge Barreto**: Conceptualization (equal); Funding acquisition (lead); Project administration (supporting); Resources (supporting); Supervision (supporting); Writing – original draft (supporting); Writing – review & editing (supporting). **Imad I. Faruque**: Conceptualization (equal); Data curation (equal); Formal analysis (equal); Investigation (equal); Methodology (equal); Project administration (lead); Supervision (lead); Writing – original draft (equal); Writing – review & editing (lead).

DATA AVAILABILITY

The data that support the findings of this study are available from the corresponding author upon reasonable request.

REFERENCES

[1] M. D. Hughes, B. Lekitsch, J. A. Broersma, and W. K. Hensinger, "Microfabricated ion traps," Contemp. Phys. **52**, 505–529 (2011).
[2] Z.-S. Yuan, X.-H. Bao, C.-Y. Lu, J. Zhang, C.-Z. Peng, and J.-W. Pan, "Entangled photons and quantum communication," Phys. Rep. **497**, 1–40 (2010).
[3] J. Wang, F. Sciarrino, A. Laing, and M. G. Thompson, "Integrated photonic quantum technologies," Nat. Photonics **14**, 273–284 (2020).
[4] H.-L. Huang, D. Wu, D. Fan, and X. Zhu, "Superconducting quantum computing: A review," Sci. China Inf. Sci. **63**, 180501 (2020).
[5] X. Chen, C. Li, and H. K. Tsang, "Device engineering for silicon photonics," NPG Asia Mater. **3**, 34–40 (2011).
[6] L. Caspani, C. Xiong, B. J. Eggleton, D. Bajoni, M. Liscidini, M. Galli, R. Morandotti, and D. J. Moss, "Integrated sources of photon quantum states based on nonlinear optics," Light: Sci. Appl. **6**, e17100 (2017).
[7] B. M. Burridge, I. I. Faruque, J. G. Rarity, and J. Barreto, "Integrate and scale: A source of spectrally separable photon pairs," Optica **10**, 1471–1477 (2023).
[8] J. B. Christensen, J. G. Koefoed, K. Rottwitt, and C. J. McKinstrie, "Engineering spectrally unentangled photon pairs from nonlinear microring resonators by pump manipulation," Opt. Lett. **43**, 859–862 (2018).

[9]B. M. Burridge, I. I. Faruque, J. G. Rarity, and J. Barreto, "High spectro-temporal purity single-photons from silicon micro-racetrack resonators using a dual-pulse configuration," Opt. Lett. **45**, 4048–4051 (2020).

[10]L. G. Helt, Z. Yang, M. Liscidini, and J. E. Sipe, "Spontaneous four-wave mixing in microring resonators," Opt. Lett. **35**, 3006–3008 (2010).

[11]I. I. Faruque, B. M. Burridge, M. Banic, M. Borghi, J. E. Sipe, J. G. Rarity, and J. Barreto, "Quantum-referenced spontaneous emission tomography," Quantum Sci. Technol. **8**, 045024 (2023).

[12]M. Liscidini and J. E. Sipe, "Stimulated emission tomography," Phys. Rev. Lett. **111**, 193602 (2013).